Using a Water Lens for Light Concentration in Thermoelectric Generation

Keita O. Ito[1], Hongtao Sui[1], Hidetoshi Hakozaki[2], Hiroshi Kinoshita[2], and Ryosuke O. Suzuki[1, 3]

[1]Division of Materials Science and Engineering, Faculty of Engineering, Hokkaido University.

[2]Department of Mechanical Engineering, Fukushima National College of Technology.

[3]CREST (Core Research of Evolutional Science & Technology) researcher, Japan Science and Technology Agency (JST).

Abstract

A water lens is employed to concentrate sunlight on the surface of a thermoelectric (TE) module in order to heat it. This water lens can change its shape flexibly and adjustable to solar altitudes. The lens shape and light path were simulated for the cases when the light is incident at an angle to the water surface, parallel to the central axis of the half-cylindrical water lens, and when the light is focused on a plate. A condensing ratio larger than 70 is achieved when the incident light is closer to

the normal of the water surface and if the optimal lens shape is maintained.

Key words: thermoelectric generation; water lens; condensing ratio; light path simulation

1. Introduction

Solar energy represents a clean source of energy and power generation using solar cells has been widely studied. Solar cells can effectively convert solar energy into electricity in a wavelength range between the ultraviolet and visible light. However, the power generation of a solar cell in the infrared region, where about 50% of solar energy exists, is less effective. Therefore, infrared ray is separated for solar cells using a wavelength selection filter, and the residual light was used as a heat source for thermoelectric power generation.[1-3]

The output of thermoelectric power generation is generally proportional to the square of the temperature difference at the two element terminals. Therefore, in order to generate electricity using the heat source with a low energy density such as solar heat, it is necessary to condense the heat. However, because the altitude of the sun changes as the earth rotates and revolves around the sun,

the stable keeping of the good condition for heat condensation is not straightforward. The sunlight tailing system,[4, 5] by which the position and direction of the lens are changed, has been conventionally used to condense the solar heat, but this system requires mechanically complicated actuators. Traditionally, the condensing methods using a trough[6, 7] and a tower have been employed, equipping with a large-scale mechanical movements. Here, we will investigate the positive usage of water refraction as a simple method of condensing heat. It is easy to invest in construction of the water lens because its components, water and a plastic sheet, are inexpensive and easily obtained all over the world. The shape of the water lens can be adjusted to variations in solar altitudes without moving the focusing position or direction of the lens.

In this paper, using numerical simulations and experiments, we examine the feasibility of the water lens as a condenser. The best condition is searched using the optical simulation of light path in the water lens, and its applicability as solar light-thermoelectric conversion is evaluated. Some challenging works using water and vinyl sheet were reported previously as try-and-error base, however, the precise analysis based of the lens shape and the focus distance has never conducted.

The purpose of this work is to show the condensing ability of water lens and the possible

applicability for solar light-thermoelectric conversion. For simple example in analysis, a half-cylindrical water lens is taken here.

2. Shape of the Water Lens

To simplify the geometrical analysis, a half-cylindrical water lens is considered in a two-dimensional cross-section, as shown in Fig. 1. The shape of the water lens is firstly determined as a function of the mass of water and the tension applied to both ends of the transparent sheet. Fig. 2 shows a cross-sectional view of the transparent sheet and water surface, where the balance of forces is analyzed at the position marked as (CHF). F_i and F_g are the forces on the plane marked as HF resulting from water pressure and the weight applied to the water at CHF, respectively. Considering the force balances in both the x and y directions, the following formulae can be derived.

$$1/2\rho g f^2(x_F) + T_0 = T_F \cos\theta \tag{1}$$

$$T_F \sin\theta + \int_{x_F}^{x_C} \rho g[-f(x)]dx = 1/2mg \tag{2}$$

Here, ρ, g, and m are the density of water, acceleration of gravity, and total mass of water in the lens, respectively. T_0, T_F, and $f(x)$ are the horizontal tension at the end of sheet, the tension at the point F,

and a function describing the apparent shape of the sheet, respectively. The origin is set to be at the center of the cylindrical water surface, and y represents the vertical position of the water surface. Here, the z-axis is neglected under the assumption of two-dimensional symmetry. θ is the slope of the sheet at the point F, whose coordinate is (x_F, $f(x_F)$). x_C is the horizontal position of the water edge.

From these two equations and the boundary condition as $f'(x_c) = mg/(2T_0)$, the following differential equation is obtained.

$$f'(x) = \sqrt{-1 + \frac{(mg)^2 + (2T_0)^2}{\left(2T_0 + \rho g y^2\right)^2}} \tag{3}$$

The shape of the lens can be determined by solving this differential equation; however, it is difficult to solve eq. (3) analytically. Therefore, the lens shape is found using a numerical solution, as shown below. First, h is set to the y-coordinate at the bottom of the water lens and this value is calculated from the boundary condition, $f'(0) = 0$, because the slope of the plastic sheet is set as being horizontal at the bottom of the lens.

$$h = -\sqrt{\frac{\sqrt{(mg)^2 + (2T_0)^2} - 2T_0}{\rho g}} \tag{4}$$

Then, $f(x)$ is solved numerically. h is divided into the segments with equal-sized interval along the

y-axis, and the slope of the segments is calculated from eq.(3).

Fig. 3 illustrates the numerical results for $f(x)$, where N is the number of interval. By increasing N, the more smooth outline of the water lens was evaluated. For the calculations hereafter, N was normally set to 1,000.

3. Light Path

As shown in Fig. 4, a beam of light enters the water. The incident and refraction angles are denoted as θ_1 and θ_2, respectively. The relative refraction index, n, is defined by Snell's law as

$$n = \frac{\sin\theta_1}{\sin\theta_2} \tag{5}$$

This can be also applied at the bottom of the water lens, where the slope of the vinyl sheet should be 0. In order to use eq. (5), the angles of light, θ_2 and ψ, at the incident point to the plastic sheet are converted to the new angles, θ_3 and φ, as illustrated in Fig. 5. θ_3 is the incident angle to the sheet, and ψ is the angle between the x-axis and the tangential line on the tangential plane. φ represents the angle between the z-axis and the optical projection when the refracted light is projected onto the sheet.

$$\theta_3 = \arccos\left(\cos\phi\cos\theta_2\right) \tag{6}$$

$$\varphi = \arcsin\left[\frac{\cos\theta_2 \sin\psi}{\sqrt{\left(\cos\theta_2 \sin\psi\right)^2 + \sin^2\theta_2}}\right] \tag{7}$$

Since the incident angle to the plastic sheet, θ_3, is known, the refraction angle θ_4 in vinyl can be obtained using Snell's law. Additionally, at the bottom part of the water lens, the light travels from water to air, and total internal reflection occurs when

$$\theta_3 > \arcsin\left(1/n\right) \tag{8}$$

The reflected light will not arrive at the focusing point as we expected. Here, the light paths after total reflection are not traced for simplicity.

4. Simulation of Energy Condensation

When light is condensed by a water lens, an attenuation of energy occurs as a result of the reflection at the two interfaces, and partially of the total reflection at the bottom of the lens. In addition, optical absorption in water also occurs.[9] However, the optical absorption has been disregarded here because the distance of water through which the light passes is very short and the

optical absorption of water is much smaller than the energy loss at the interfaces. When light enters into a highly transparent substance such as water or plastic sheet, the ratio of unreflected energy penetrating the two interfaces is determined as follows.[10]

$$\eta_1 = \frac{\sin 2\alpha \sin 2\beta}{\sin^2(\alpha+\beta)\cos^2(\alpha-\beta)} \tag{9}$$

$$\eta_2 = \frac{\sin 2\alpha \sin 2\beta}{\sin^2(\alpha+\beta)} \tag{10}$$

Here, α and β are the incident angle and the refraction angle at the two interfaces, respectively. η_1 and η_2 are the transmissivities of the light oscillating perpendicularly and parallel to the incident plane, respectively. The transmissivity of light entering normal to the water surface is given by

$$\eta = \frac{4n}{(1+n)^2} \tag{11}$$

These expressions are known as the Fresnel equations.[9] The amount of energy condensed on the receiver is calculated by combining these expressions and the light path deduced in the previous section.

5. Experimental Results of Light Condensation

To investigate whether our calculation can correctly simulate the focusing property of the water

lens, experiments were also conducted for comparison. The water lens was prepared using a 1.0-mm-thick and 190-mm-wide vinyl sheet. 4.0 kg water per 1 meter width of the sheet was precisely measured and filled as the media of lens. The wind-up roll at the terminal of sheet was pulled by using two spring gauges, and the horizontal tension to the sheet was controlled. Because the fine distortion of the sheet was critical to the final lens form, the sheet was finely tuned after removing the springs. The distribution of the condensing ratio was measured by using the quasi-parallel light normal to the water lens. The artificial light was generated by a slide projector for screen presentation, controlled to become parallel by a plastic Fresnel lens, and irradiated to the water lens by a mirror. The light intensity was measured using a photo diode with a light-receiving width of 2.7 mm, and the condensing ratio was calculated from the ratio of the electromotive force (EMF of photo diode) with and without the water lens. The EMF value showed a good linearity against the illumination of light source as reported in the previous paper[8], and the open circuit voltage was taken as the measure of light intensity. Fig. 6 shows a profile of the condensing ratio obtained in these experiments. The measurements were performed at 2.0-mm intervals by shifting the light-receiver by 10-mm height intervals below the lens. Although the lens was symmetrical and

the artificial lamp radiated perpendicularly just above the lens, the measured distribution was slightly asymmetric. As a result of the finite size of the receiver (2.7 mm), the sharp condensation effect was smeared out, as can be seen in Fig. 6. The maximum was found at (x, d) = (0 mm, -350 mm) with the highest condensing ratio being 4.48.

6. Simulation Results of Light Condensation

Fig. 7 shows the light path and the condensing ratio obtained from the simulation using the same conditions as those in the experiment shown in Fig. 6. Here the condensing ratio was defined as the ratio of the integrated intensity on the condensing board and the irradiated intensity to the water surface. The integrated energy was evaluated by numerical integration as the total energy irradiated on the condensing board. The integrated intensity was then calculated by dividing the integrated energy by the surface area of the condensing board. To obtain a smooth lens shape in the numerical calculation here, the number of intervals, N, was set to 100,000. The energy loss was considered using the Fresnel's equations. Fig. 7 (a) shows the simulated light paths, and the painted area in violet shows the region in which the condensation ratio was calculated. This area corresponds to the

experimental limits of movement in the x-direction. This is because the area covered in the experiments was limited within 10 mm from the central axis of the lens. The simulated condensation of light was symmetrical, although a small deviation can be seen within the error of the 2-dimensional expression. The maximum condensing ratio is about 19, as seen at the position (x, d) = (0 mm, -320 mm).

Comparison with Figs. 6 and 7 (b) shows that the simulated and measured condensing-ratio distributions agreed relatively well. However, because the condensing width in the simulation was narrower than the experimental width, the condensing ratio in the simulation was evaluated about 4-times higher than that in the experiment. This difference may be attributed to experimental errors such that a perfect parallel beam can not be realized by the artificial lamp and that the shape of the water lens deviates slightly. Unwillingly the additional strain along the lens axis lens was given because the inhomogeneous tensile stress remained in the transparent sheet. Although real light contains a spectrum of wavelength, our simulation neglected chromatic aberration. Because the lens shape was small and differences of light path due to differences of wavelength could be neglected, the simulation was performed by assuming a monochromatic light source and the refractive index as

1.333. These assumptions may be the reasons of the discrepancy between Figs. 6 and 7 (b).

7. Oblique Incidence

Since the solar altitude shifts during the day, oblique incident beams must be considered. A simulation was performed on the focusing property assuming that light is radiated from the z-axis direction toward the water surface. The incident angle to the water surface is set to θ_1. The lens shape was controlled by changing the angle γ, as shown in Fig. 8. γ is the angle of the tension applied to both ends of the plastic sheet against the water surface. The mass of water was kept constant at 4 kg per meter.

Fig. 9 shows some examples of the simulated results under these conditions. In the calculation, the width of the receiver was assumed to be 2.7 mm. The results are very sensitive with respect to the shape of the water lens; a sharp peak exists in the condensing ratio. Therefore, the tension should be optimized reflecting γ. When the light irradiates the water perpendicularly to its surface ($\theta_1 = 0$), the condensing ratio approached to 54 at $\gamma = 36°$, and it decreased when γ was not set to be this optimum value. The maximum condensing ratio was nearly constant for θ_1 in the range 0 to 70°, and the

optimum γ value to obtain this condensation decreased as θ_1 increased. The maximum condensing ratio decreased below 50, however, when θ_1 was greater than 70°. This was because the total internal reflection occurred at the bottom part of the water lens. In order to concentrate oblique incident beams, (i.e., large θ_1 values), the angle γ should be controlled to be smaller. This shows that thin lenses behave more favorably for oblique incident beams.

8. Experimental Results of TEG with Oblique Incidence

The sunlight radiating from z-direction slantly to the water surface was condensed onto a 23-pairs TE module (6 × 8 mm^2), and its TE motive force V from Bi-Te elements was monitored. The water lens designed in Section 5 was used. Fig.10 shows the condensation of solar light at Sapporo. One surface of the TE module was kept at 283 K with the water-cooled copper plate (Cooling water circulated by flow rate of 9 L/min). The thermal resistance to the water-cooled plate was minimized by painting the thermal conductive grease on the interface thinly. The black body tape was stuck on the other surface to minimize the reflection at the surface. Because the solar position varies every moment, the maximum TE motive force was investigated at only a constant height by fixing the

position of TE module using a jack.

At the time when the maximum of TE motive force V could be obtained, V and V_0 were measured with and without the lens, respectively. Heat condensing ratio, C_h, is defined as the ratio, V / V_0. The incident intensity of solar light, U_0, was obtained as a function of time from the daily report at Sapporo local office, Japan Meteorological Agency. The altitude of the sun γ_S (= $\pi/2-\theta_1$) was evaluated using the geological position method. [11-14] Although, the exact time based on the noon sun time could not be substituted to the equation used for the evaluation of γ_S, the difference from actual condition was as small as 0.3 degree, and ignored in this work. When the time passed, both V and C_h decreased as shown in Fig.11. At 14:15, the maximum temperature difference of about 9 K was obtained by the measurement with water lens condensing.

Fig.12 shows the comparison of C_h and C, where C was calculated from γ_S. C_h decreases gently as γ_S decreases. C decreases rapidly when $\gamma_S > 42°$. This is because the condensing width of the light became larger than the width of the TE module (6mm) as shown in Fig. 12. It is satisfactory that the condensing light is as wide as the size of TE module.

9. Conclusion

A water lens consisting of water and a transparent sheet was investigated. Using the mechanical force balance, a differential equation describing the shape of the water lens was solved numerically. The light paths were evaluated to determine the condensing ratio. The ratios in some cases were as high as 18, while the corresponding experiments showed that the ratio achieved to the maximum values of 4. As the focal point can be well predicted, some experimental tuning could lead to the higher values.

From the simulation in which the light irradiates the water surface obliquely, the high condensing ratios of about 60 can be achieved by adjusting γ or the tension to their optimum values. When the incident angle is the larger, the thinner lens is favorable. Adjusting the shape of a thin lens can greatly enhance the condensing ratio.

From the experiment of TE generator under the solar light, it is satisfactory that the condensing light width is as large as the width of TE module.

Acknowledgment

The authors thank Prof. K. Koumoto at Nagoya University and Dr. R. Funahashi at AIST-Kansai for their kind discussions. This work is financially supported by JST-CREST and JSPS Grant-in-Aid for Exploratory Research (No.24656574). One of the authors (HTS) thanks the China Scholarship Council for sponsoring his stay in Japan.

References

[1] N. Wang, L. Han, H. He, N.H. Park and K. Koumoto, Energy Environ. Sci. 4, 3676 (2011).

[2] X. Ju, Z. Wang, G. Flamant, P Li and W. Zhao, Sol. Energy 86, 1941 (2012).

[3] Y. Deng, W. Zhu, Y. Wang and Y. Shi, Sol. Energy 88, 282 (2013).

[4] V. Poulek and M. Libra, Solar Energy Materials and Solar Cells 51, 113 (1998).

[5] B.J. Huang, W.L. Ding and Y.C. Huang, Sol. Energy 85, 1935 (2011).

[6] T. Tao, Z. Hongfei, H. Kaiyan and A. Mayere, Sol. Energy 85, 198 (2011).

[7] Q. C. Murphree, Sol. Energy 70, 85 (2001).

[8] R. O. Suzuki, A. Nakagawa, H. Sui, and T. Fujisaka, Journal of Electronic Materials, 42, (7) 1960 (2013).

[9] E. O. Hulburt, Journal of the Optical Society of America 35, 698 (1945).

[10] J. F. Wu and C. M. Zhang, Optik 121, 1835 (2010).

[11] E. Elvegård and G. Sjöstedt, Illuminating Engineering 35, 333 (1940).

[12] M. G. Davies, Building and Environment 43,1421 (2008).

[13] R. E. Parkin, Sol. Energy 84, 912 (2010).

[14] R. Kittler, S. Darula, Sol. Energy 93, 72 (2013).

Figure Captions

Fig. 1 Three dimensional modeling of the water lens.

Fig. 2 Balance of forces at a part of water lens.

Fig. 3 Lens form computed from the numerical solution. Number of division, *N*, is (a)5, (b)10, (c)20 and (d)1,000.

Fig. 4 Refraction on the water surface.

Fig. 5 Geometric relationship on refraction at the bottom part of water lens.

Fig. 6 Condensing ratio measured in the experiment.

Fig. 7 Light path and condensing distribution obtained in the simulation.

Fig. 8 Light path in case of oblique incidence, (a) three-dimensional view, (b) a view from the z-axis direction.

Fig. 9 Condensing ratio at the time of oblique incidence.

Fig. 10 Photo of experimental device.

Fig. 11 Time dependency of the incident intensity, altitude of sun, heat condensing ratio and electromotive force.

Fig. 12 Influence of the altitude of sun on heat condensing ratio, condensing ratio and width of the light.

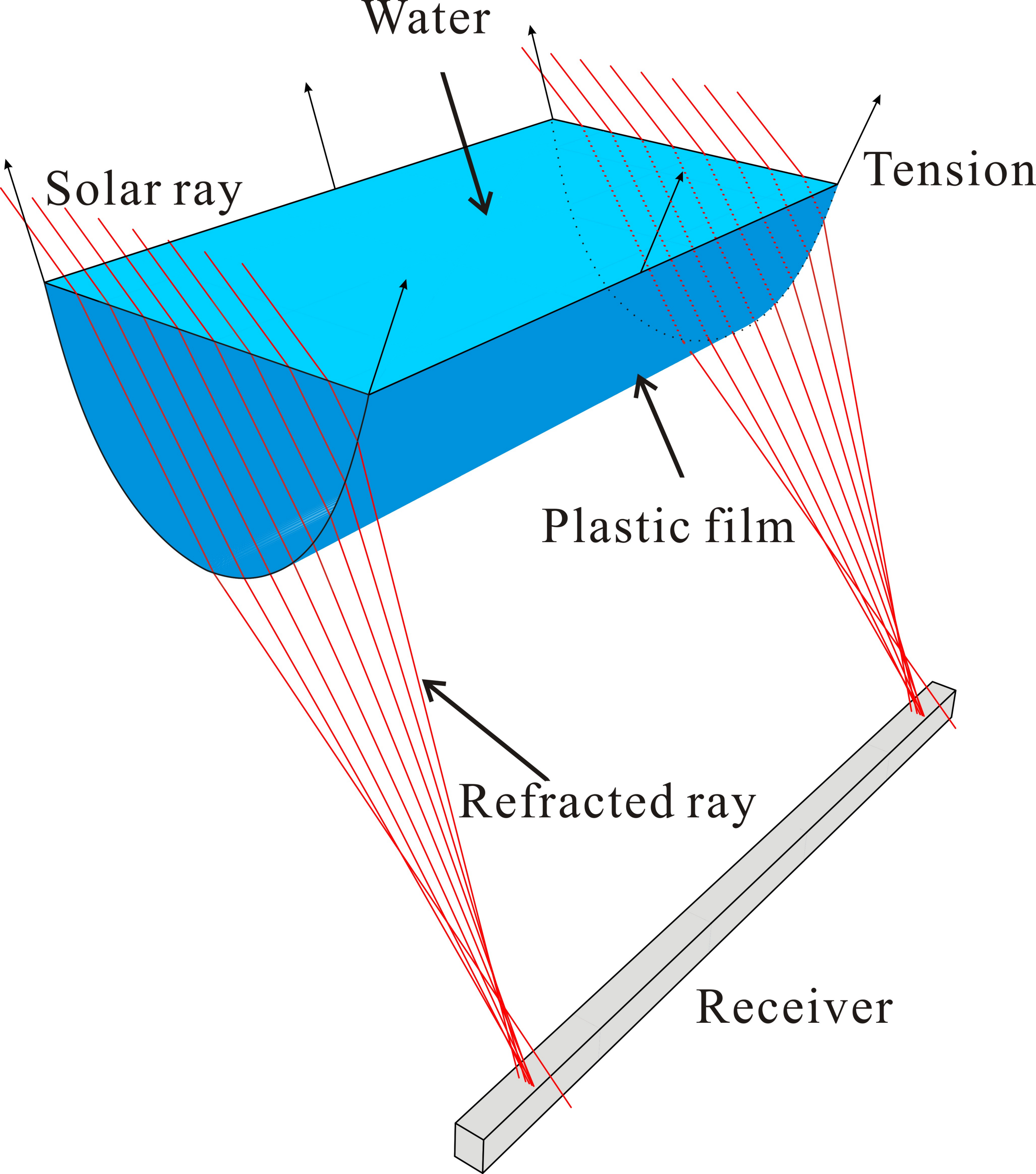
Water
Solar ray
Tension
Plastic film
Refracted ray
Receiver

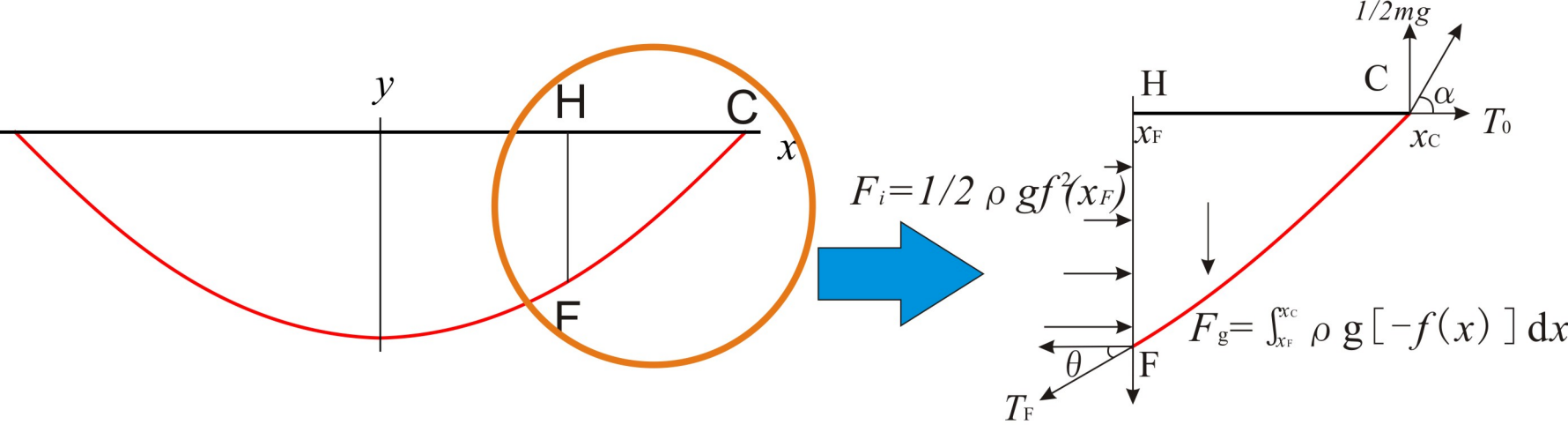
y
H
C
x
F
1/2mg
C
α
H
T0
xF
xC
Fi=1/2 ρ gf2(xF)
Fg= ∫xFxC ρ g[−f(x)] dx
θ
F
TF

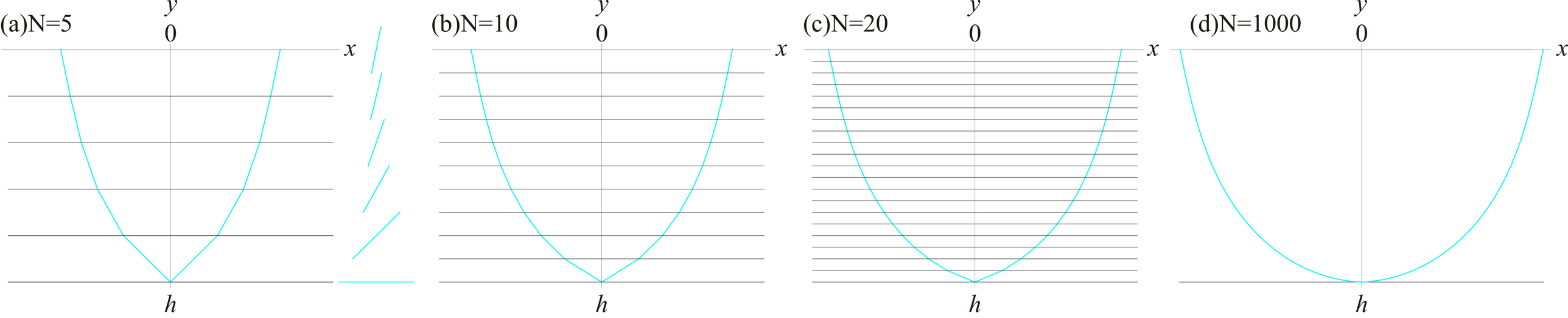
(a)N=5
y
0
x
h
(b)N=10
y
0
x
h
(c)N=20
y
0
x
h
(d)N=1000
y
0
x
h

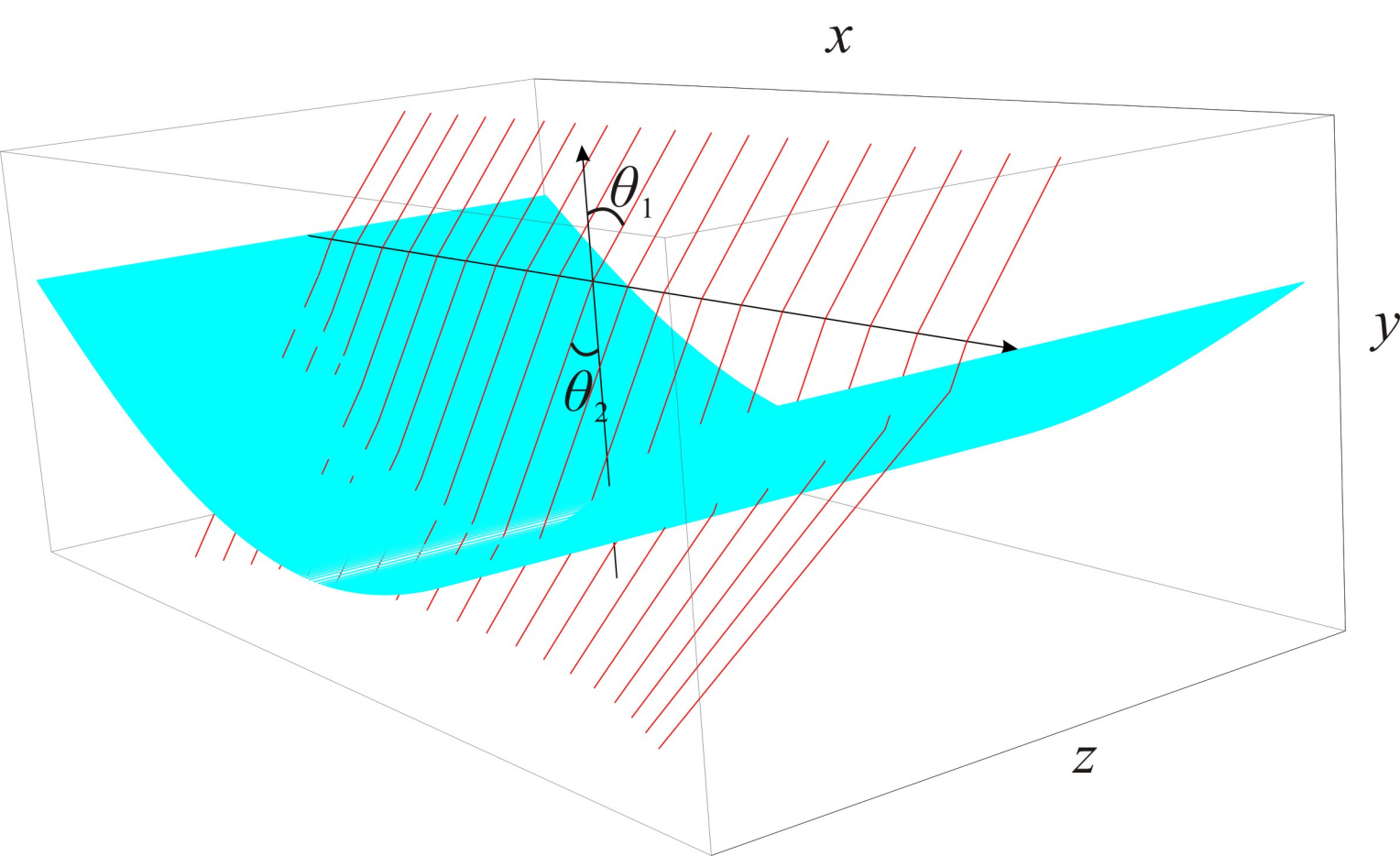
x
y
z
θ_1
θ_2

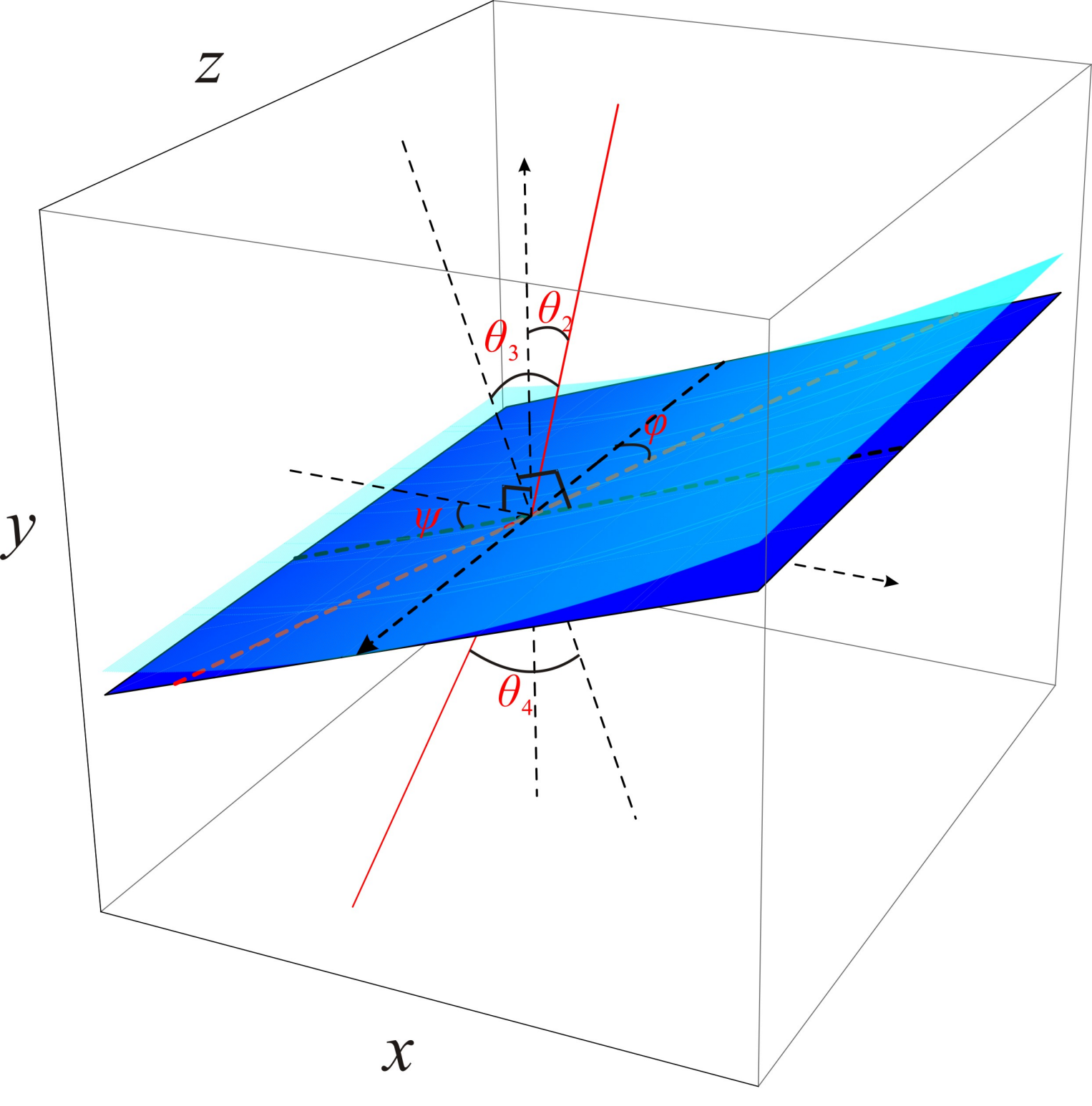
z
y
x
θ_2
θ_3
φ
ψ
θ_4

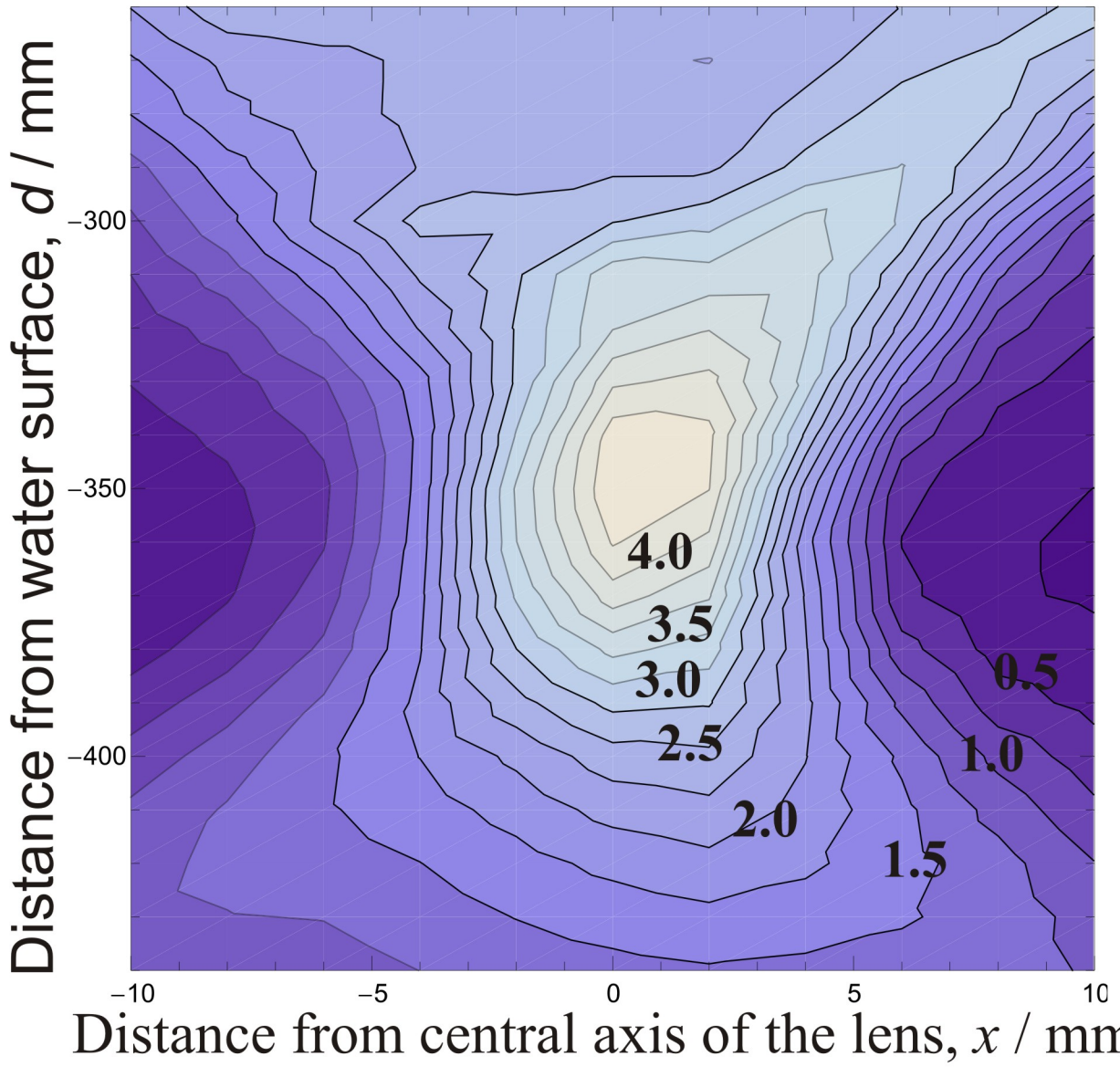
Distance from water surface, d / mm
−300
−350
−400
4.0
3.5
3.0
2.5
2.0
1.5
1.0
0.5
−10
−5
0
5
10
Distance from central axis of the lens, x / mm

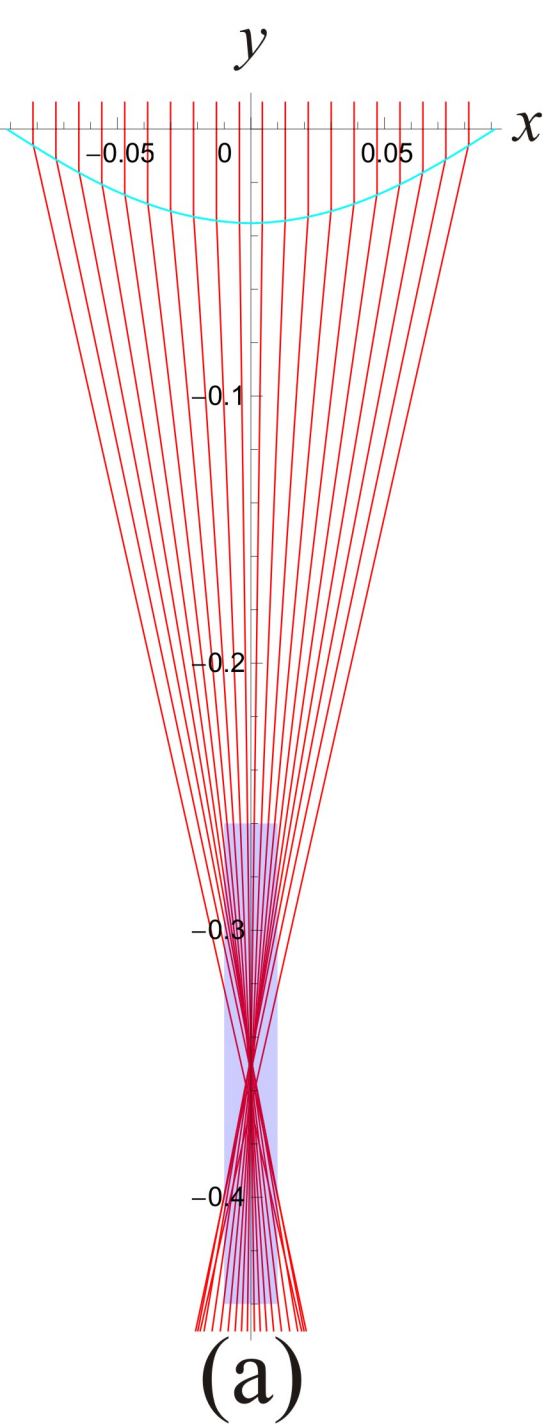
y
x
−0.05
0
0.05
−0.1
−0.2
−0.3
−0.4

(a)

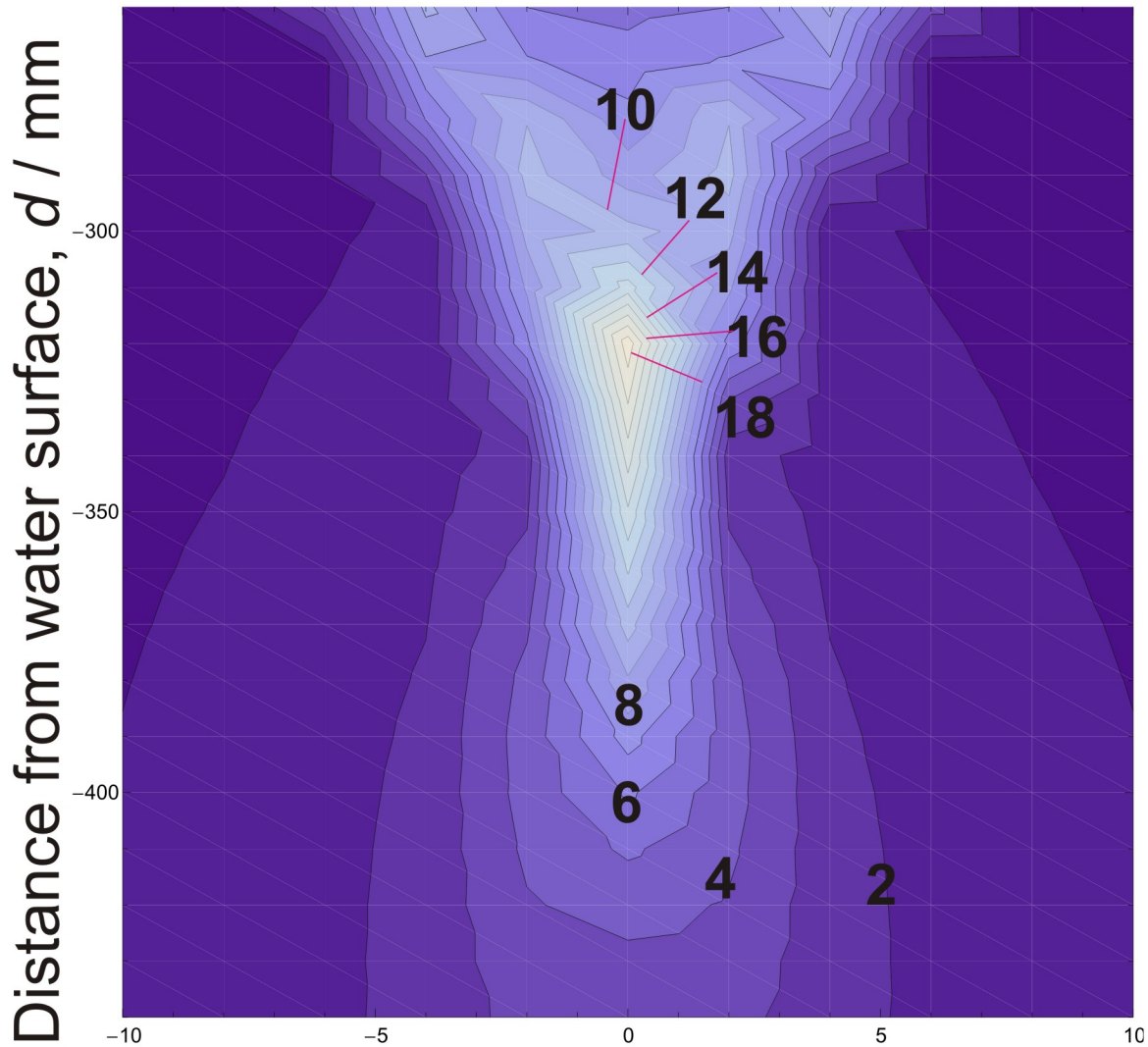
Distance from water surface, d / mm
−300
−350
−400
10
12
14
16
18
8
6
4
2
−10
−5
0
5
10
Distance from central axis of the lens, x / mm

(b)

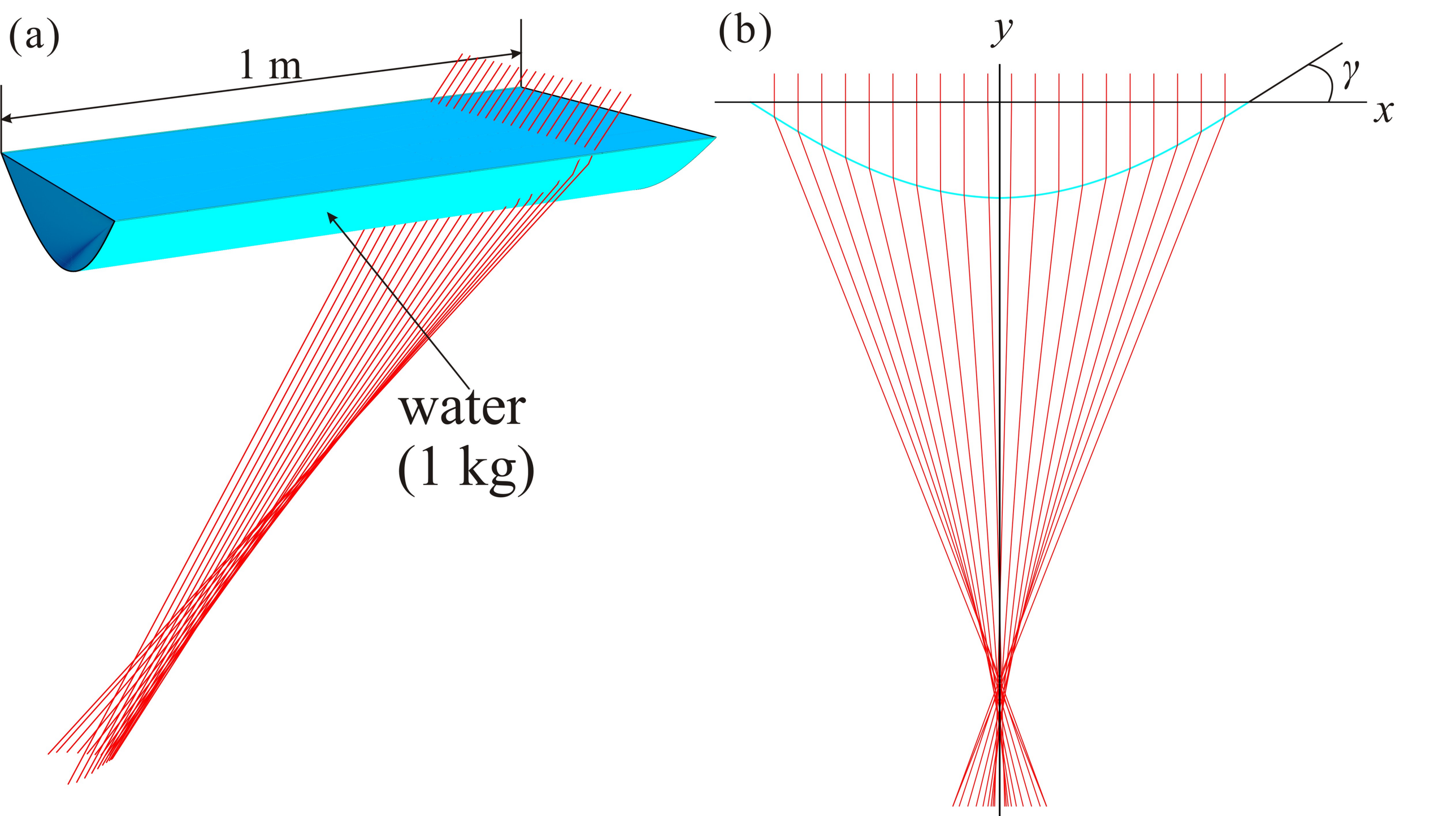
(a)
1 m
water
(1 kg)
(b)
y
γ
x

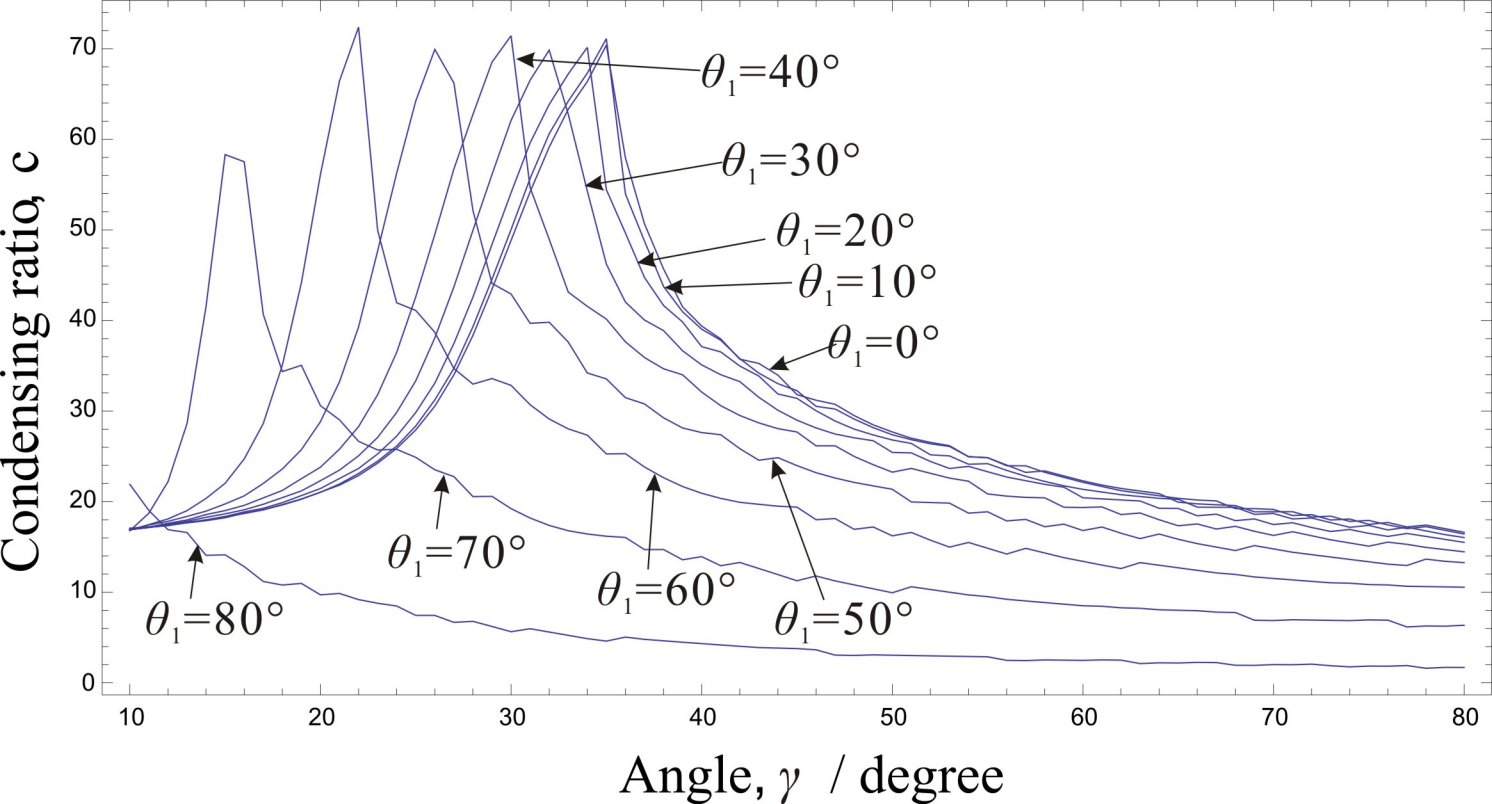
Condensing ratio, c
Angle, γ / degree
θ1=40°
θ1=30°
θ1=20°
θ1=10°
θ1=0°
θ1=70°
θ1=60°
θ1=50°
θ1=80°
0
10
20
30
40
50
60
70
80

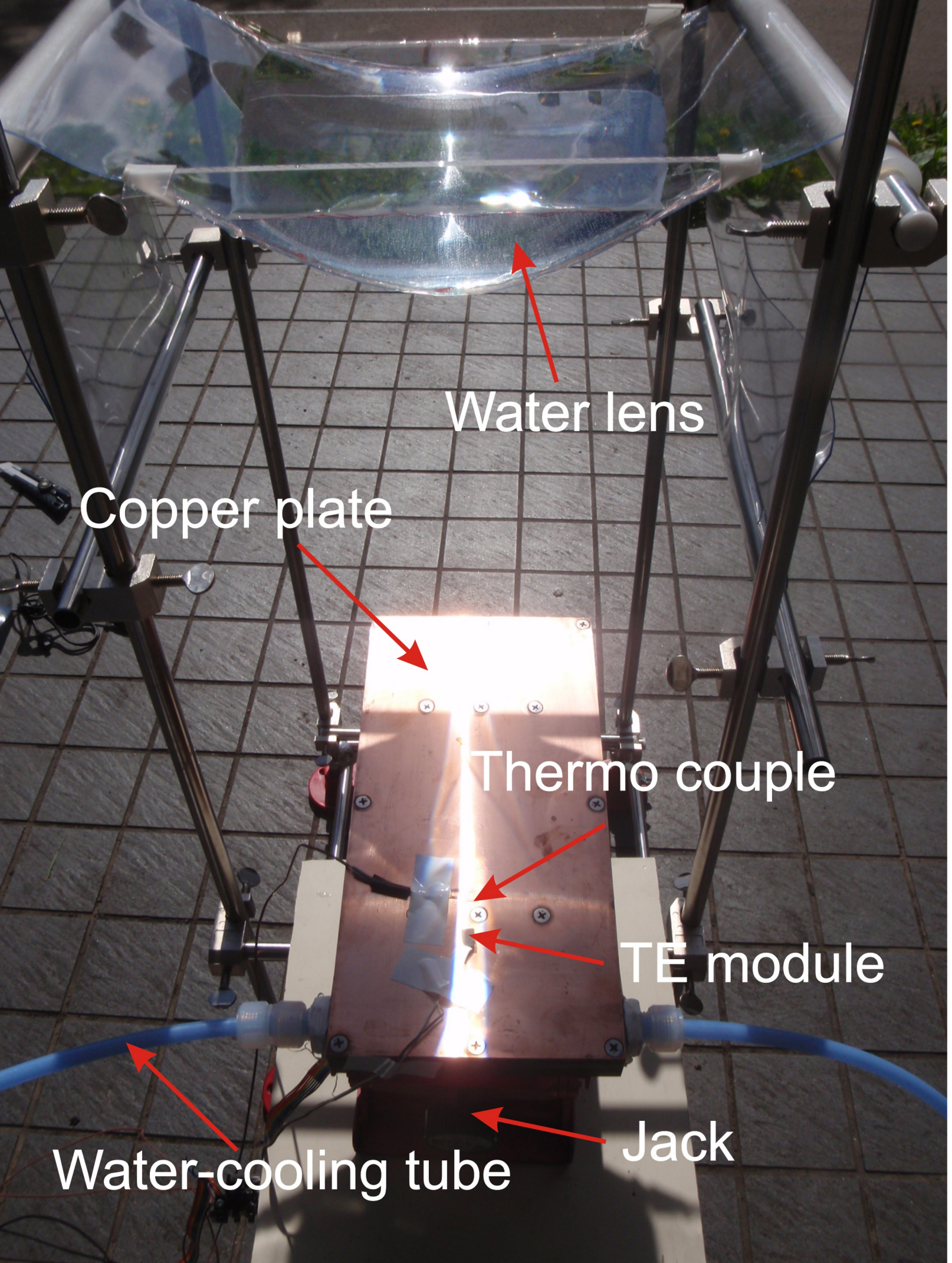
Water lens
Copper plate
Thermo couple
TE module
Jack
Water-cooling tube

Incident intensity, U_0 / W m^{-2}
900
850
800
750
700
Heat condensing ratio, C_h
5.4
5.2
5
4.8
4.6
4.4
4.2
Altitude of sun, γ_S / degree
60
50
40
30
20
10
0
Electromotive force, V / mV
90
80
70
60
50
40
30
20
10
0
14 :13
14 :28
14 :52
15 :07
15 :13
Time, t

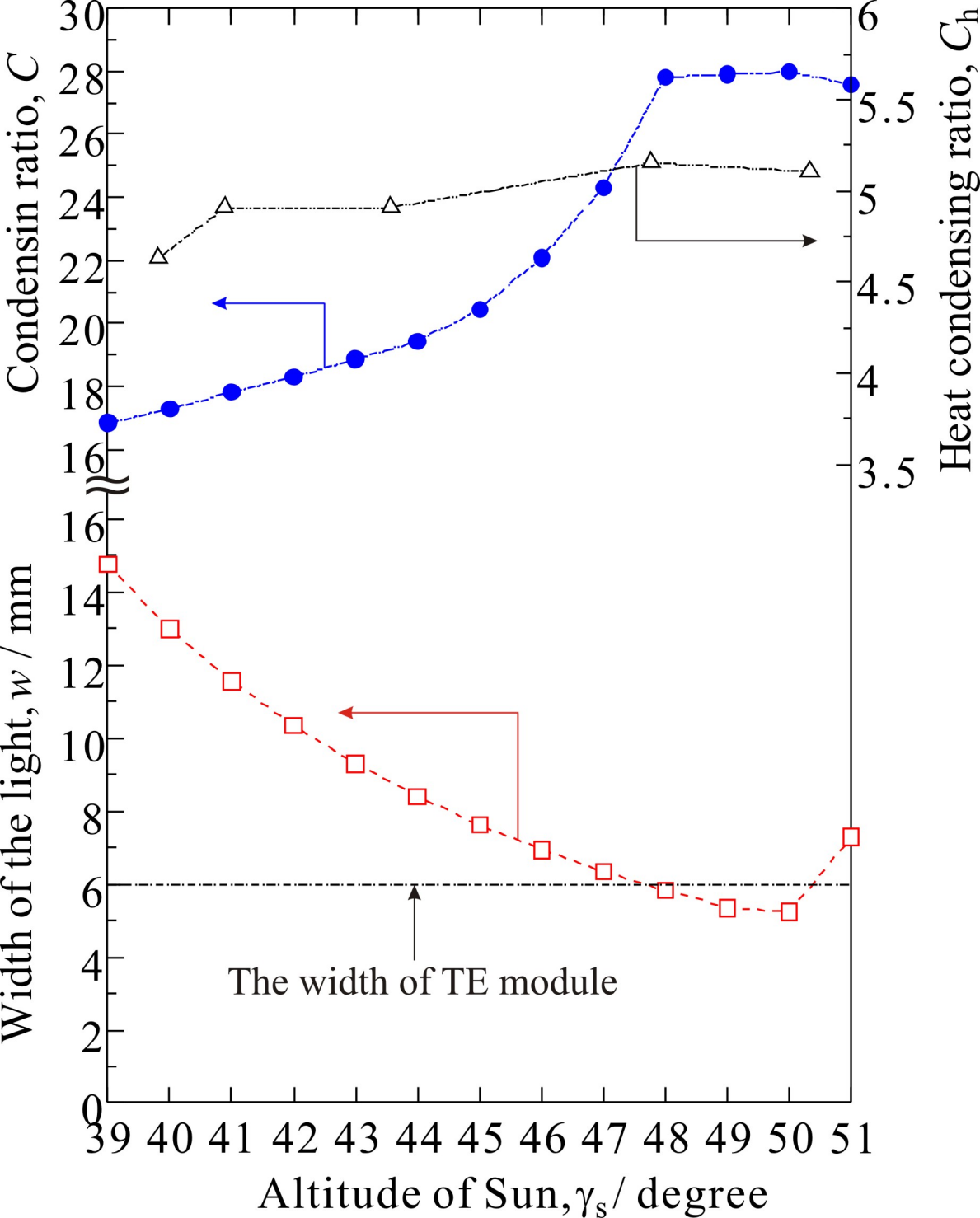
Condensin ratio, C
Heat condensing ratio, C_h
Width of the light, w / mm
The width of TE module
Altitude of Sun, γ_s / degree
30
28
26
24
22
20
18
16
16
14
12
10
8
6
4
2
0
6
5.5
5
4.5
4
3.5
39 40 41 42 43 44 45 46 47 48 49 50 51